

# Runt-Related Transcription Factor RUNX3 Is a Target of MDM2-Mediated Ubiquitination

Xin-Zi Chi,<sup>1</sup> Jiyeon Kim,<sup>1</sup> Yong-Hee Lee,<sup>1</sup> Jung-Won Lee,<sup>1</sup> Kyeong-Sook Lee,<sup>1</sup> Heejun Wee,<sup>1</sup> Wun-Jae Kim,<sup>2</sup> Woo-Yoon Park,<sup>3</sup> Byung-Chul Oh,<sup>4</sup> Gary S. Stein,<sup>5</sup> Yoshiaki Ito,<sup>6</sup> Andre J. van Wijnen,<sup>5</sup> and Suk-Chul Bae<sup>1</sup>

Departments of <sup>1</sup>Biochemistry and <sup>2</sup>Urology, College of Medicine, Institute of Tumor Research, Chungbuk National University; <sup>3</sup>Department of Radiation Oncology, Chungbuk National University College of Medicine, Cheongju, South Korea; <sup>4</sup>Lee Gil Ya Cancer and Diabetes Institute, Gachon University of Medicine and Science, Incheon, South Korea; <sup>5</sup>Department of Cell Biology and Cancer Center, University of Massachusetts Medical School, Worcester, Massachusetts; and <sup>6</sup>Institute of Molecular and Cell Biology, Proteos, Singapore, Singapore

## Abstract

**The p14<sup>ARF</sup>-MDM2-p53 pathway constitutes an effective mechanism for protecting cells from oncogenic stimuli such as activated *Ras* and *Myc*. Importantly, *Ras* activation induces p14<sup>ARF</sup> and often occurs earlier than p53 inactivation during cancer development. Here, we show that RUNX3, a tumor suppressor in various tumors including stomach, bladder, colon, and lung, is stabilized by *Ras* activation through the p14<sup>ARF</sup>-MDM2 signaling pathway. RUNX3 directly binds MDM2 through its Runt-related DNA-binding domain. MDM2 blocks RUNX3 transcriptional activity by interacting with RUNX3 through an acidic domain adjacent to the p53-binding domain of MDM2 and ubiquitinates RUNX3 on key lysine residues to mediate nuclear export and proteasomal degradation. Our data indicate that the lineage-specific tumor suppressor RUNX3 and the ubiquitous p53 protein are both principal responders of the p14<sup>ARF</sup>-MDM2 cell surveillance pathway that prevents pathologic consequences of abnormal oncogene activation.** [Cancer Res 2009;69(20):8111–9]

## Introduction

Deregulation of proliferation in mammalian cancer cells involves the synergistic induction of promotogenic regulatory pathways and inactivation of antimitogenic factors. The regulatory functions of the two classic tumor suppressors, p53 and retinoblastoma protein (pRB), are well understood. Accumulating evidence indicates that the cell fate-determining Runt-related (RUNX) transcription factors play complementary biological roles to the p53 and pRB tumor suppressors in both hematopoietic and nonhematopoietic cancers, including cancers of the gastrointestinal tract as well as breast and prostate (1). Although tumor-related modifications in the p53-pRB network are evident in the same spectrum of tumors, a fundamental question is whether and how RUNX-responsive regu-

latory pathways are mechanistically linked to p53-pRB-dependent cellular surveillance mechanisms.

Several oncogenic and DNA damage-related pathways converge on p53, which is the key effector of a critical checkpoint that arrests the cell cycle (2). The p53 protein is normally labile and maintained at very low levels. Mouse double minute 2 (MDM2; HDM2 in human, called here MDM2), a RING finger E3 ubiquitin ligase, plays an essential role in p53 degradation by promoting ubiquitination of p53, which induces nuclear export and proteasomal degradation of p53 (3). The stabilization of p53 and its activation is mediated by the p14<sup>ARF</sup> (human)-p19<sup>ARF</sup> (mouse)/MDM2 pathway in response to oncogenic stimulation or by DNA damage-dependent activation through the ATM/ATR kinase pathway (4). p14<sup>ARF</sup> inhibits the ubiquitin ligase activity of MDM2 by binding to a central region of MDM2. MDM2 can also inhibit p53-mediated transcriptional activation in a ubiquitination-independent manner (5). MDM2 also has p53-independent functions as reflected by elevation of MDM2 activity in patients with p53 mutations (6, 7) and MDM2-mediated growth advantage in the absence of p53 (8, 9).

RUNX transcription factors play pivotal roles in normal development and neoplasia (10). Deregulation of the biological functions of the three human *RUNX* family genes, *RUNX1/AML1*, *RUNX2/CBFA1*, and *RUNX3/PEBP2αC* (11), contributes to cancer. *RUNX1* is required for hematopoiesis and is genetically altered in leukemia (12–14). *RUNX2* is linked to osteogenesis (15, 16) and alterations in human *RUNX2* levels are associated with cleidocranial dysplasia (17, 18) and osteosarcoma (19). *RUNX3* is required for the development of CD8-lineage T cells (20, 21) and TrkC-dependent dorsal root ganglion neurons (22, 23). *RUNX3* is the smallest member of the RUNX family and is prototypical for the tumor-suppressive potential of these proteins (24). For example, lower levels of *RUNX3* have been shown to be causally associated with human cancers for stomach (25), bladder (26), and colon (27). Recently, *RUNX3* was also identified as one of the five most informative genes for the CpG island methylator phenotype of colorectal cancer (28).

Because p53 and RUNX3 both control cell cycle progression and apoptotic processes (25, 29, 30), we postulate that these two proteins may be controlled by the same inhibitory pathway. Our results show that RUNX3 is stabilized by oncogenic Ras-dependent induction of the p14<sup>ARF</sup>-MDM2 pathway. MDM2 interacts with RUNX3 and suppresses the transcriptional activity of RUNX3 activity by blocking its transactivation potential as well as by facilitating MDM2-mediated ubiquitination and nuclear exclusion of RUNX3. Our data reveal that RUNX3 and p53 are both connected to the MDM2 pathway. This key finding indicates that the MDM2 pathway simultaneously controls two major tumor suppressor pathways with ubiquitous (p53) and lineage-specific (RUNX3) functions.

**Note:** Supplementary data for this article are available at Cancer Research Online (<http://cancerres.aacrjournals.org/>).

X.-Z. Chi, J. Kim, and Y.-H. Lee contributed equally to this work.

Current address for J. Kim: Department of Pharmacology and Cancer Biology, Duke University Medical Center, Durham, North Carolina.

**Requests for reprints:** Suk-Chul Bae, Department of Biochemistry, College of Medicine, Institute of Tumor Research, Chungbuk National University, 410 Sung Bong-Ro, Cheongju, Chungbuk 361-763, Korea. Phone: 82-43-261-2842; Fax: 82-43-274-8705; E-mail: scbae@chungbuk.ac.kr or Andre J. van Wijnen, Department of Cell Biology and Cancer Center, University of Massachusetts Medical School, 55 Lake Avenue North, Worcester, MA 01655. E-mail: Andre.VanWijnen@umassmed.edu.

©2009 American Association for Cancer Research.

doi:10.1158/0008-5472.CAN-09-1057

## Materials and Methods

**Plasmids and antibodies.** Full-length cDNA as well as serial deletion and point mutants of *RUNX3* (NM\_004350), *MDM2* (NM\_002392), and *p14<sup>ARF</sup>* (NM\_000077), respectively, were amplified by PCR and subcloned into pCS4-3Myc or pCS4-3HA. Anti-RUNX3 (5G4) and anti-MDM2 (SMP14, D-12) antibodies were purchased from Abcam and Santa Cruz Biotechnology, respectively.

**Cell culture and transfection.** Human embryonic kidney cells (HEK-293) and HeLa cells were maintained in DMEM and MKN45 was maintained in RPMI (Life Technologies) supplemented with 10% fetal bovine serum (Life Technologies) and 100 units/mL penicillin-streptomycin (Life Technologies) at 37°C in a humidified atmosphere with 5% CO<sub>2</sub>. Cell lines were obtained from Korea Research Institute of Bioscience and Biotechnology. Transient transfection was carried out using Lipofectamine Plus reagent (Invitrogen) according to the manufacturer's instruction. The small interfering RNA (siRNA) for *MDM2* (si-MDM2: 5'-UUACAGCACCAUCA-GUAGGUACAGA-3'; Invitrogen) and *RUNX3* (si-RX3-1: 5'-AACCCUGAUGC-CAUAGACUC-3' and si-RX3-2: 5'-UGUUCUCAACCAUCUCUG-3'; Bioneer) were used for knockdown *MDM2* or *RUNX3*, respectively. Reporter assays, immunoprecipitation, and immunoblotting analysis were done as described previously (29).

**In vitro ubiquitination assay.** GST-MDM2 and His-tagged Runt domain were overexpressed in *Escherichia coli* BL21 (DE3) and purified according to standard procedures. Ubiquitination assays were carried out by adding 20 ng each of human recombinant ubiquitin-activating enzyme (E1), ubiquitin-conjugating enzyme GST-tagged UbcH5b (E2), and HA-tagged ubiquitin, 300 ng purified GST-MDM2, and 100 to 400 ng His-Runt domain in ubiquitination reaction buffer [50 mmol/L HEPES (pH 7.4), 2.5 mmol/L precoupled Mg-ATP solution, 0.5 mmol/L phenylmethylsulfonyl fluoride]. Reactions were carried out for 2 h at 37°C.

**Apoptosis assay by Annexin V staining.** HEK-293 cells were treated with *RUNX3*-specific siRNA (si-RX3-1 or si-RX3-2) or nonspecific siRNA (si-con) at 50 nmol/L with Lipofectamine RNAiMAX (Invitrogen). Twenty-four hours after siRNA treatment, the cells were transfected with *RUNX3* and/or *K-Ras-V12* expression plasmid and incubated in serum-free DMEM for 4 h. The medium was changed with 0.5% fetal bovine serum/DMEM and further cultured 44 h. The cells were harvested and treated with Annexin V-FITC and propidium iodide according to the manufacturer's instruction (FITC-Annexin V apoptosis detection Kit1; BD Biosciences, Pharmingen) and analyzed by flow cytometry using BD FACSCalibur (BD Biosciences, Pharmingen).

## Results

**Ras activation elevates RUNX3 protein levels.** Activating *K-Ras* mutations are known to modulate the p14<sup>ARF</sup>-MDM2 pathway. We examined whether an activated *Ras* mutant controls *RUNX3* protein expression. Human embryonic kidney (HEK-293) cells were transfected with a *K-Ras* mutant that is constitutively activated by a Val<sup>12</sup> mutation or an inactivating Asn<sup>17</sup> mutation. Increased expression of *K-Ras-V12* results in a dose-dependent increase in *RUNX3* protein levels, but no increase in *RUNX3* protein is observed with the *Ras-17N* mutant (Fig. 1A). Dose-dependent increases in the levels of endogenous *RUNX3* protein and known transcriptional targets of *RUNX3*, *p21<sup>WAF/CIP</sup>* and *Bim*, were also observed on exogenous expression of *K-Ras-V12* (Fig. 1B). The induction of *p21* and *Bim* by *K-Ras-V12* did not occur when *RUNX3* was depleted by *RUNX3* siRNA knockdown, suggesting an essential role for *RUNX3* in the *K-Ras-V12*-dependent induction of *p21* and *Bim* (Supplementary Fig. S1). The increase of *RUNX3* protein level appears to be independent from *RUNX3* transcription, because *RUNX3* mRNA levels are not affected by the expression of *K-Ras-V12* (Fig. 1B).

Because all three Runx proteins induce a senescence-like growth arrest in primary mouse embryonic fibroblasts in response to acti-

vated Ras (31), we examined whether the levels of *RUNX1* and *RUNX2* are also increased by *K-Ras-V12*. Interestingly, however, the levels of the *RUNX3* homologues, *RUNX1* and *RUNX2*, were not increased by *K-Ras-V12* expression (Supplementary Fig. S2) in HEK-293 cells. This result suggests that *RUNX3* is a specific target of *K-Ras-V12* at least in HEK-293 cells, and the molecular basis for this selectivity remains to be resolved. We next examined the involvement of p14<sup>ARF</sup> in the *K-Ras-V12*-induced increase of *RUNX3* levels. Forced expression of *K-Ras-V12* or p14<sup>ARF</sup> in A549 lung cancer cells, which do not express p14<sup>ARF</sup>, increases *RUNX3* only modestly and expression of both genes further increased the levels of *RUNX3* protein (Fig. 1C).

Annexin V-FITC and propidium iodide staining followed by flow cytometric analysis revealed that transient expression of *K-Ras-V12* or *RUNX3* alone in HEK-293 cells increased the number of apoptotic cells to twice that of mock-treated cells (Fig. 1D). Coexpression of *K-Ras-V12* and *RUNX3* further increased the number of apoptotic cells by ~2-fold. Importantly, treatment of *RUNX3* siRNA abolished the increase of apoptosis by *K-Ras-V12* (Fig. 1D). Knockdown of *RUNX3* by specific siRNAs is shown in Supplementary Fig. S1. These data together suggest that *RUNX3* is a component of an oncogene surveillance pathway that prevents pathologic consequences of abnormal oncogene activation.

**MDM2 interacts with RUNX3.** Because the predicted effect of elevating p14<sup>ARF</sup> is inhibition of MDM2, the E3 ubiquitin ligase that is the principal attenuator of p53 protein levels (32), we postulated that MDM2 may also directly minimize protein expression of *RUNX3* through physical interactions between *RUNX3* and MDM2. We coexpressed epitope-tagged HA-*RUNX3* or HA-p53 and Flag-MDM2 proteins in HEK-293 followed by coimmunoprecipitation and immunoblotting (immunoprecipitation-Western blot analysis). The results show that MDM2 is present in immunoprecipitates obtained with anti-HA (*RUNX3*) antibody (Fig. 2A). Comparable amounts of MDM2 are detected in anti-HA (p53) precipitates, suggesting that MDM2 physically interacts with both *RUNX3* and p53 (Fig. 2A). The interactions between endogenously expressed *RUNX3* and MDM2 were examined in HEK-293 cells that produce two main MDM2 isoforms (90 and 75 kDa). Lysates were analyzed by immunoprecipitation with a specific *RUNX3* monoclonal antibody (5G4) followed by immunoblotting with anti-MDM2 or anti-*RUNX3* antibody. The results establish that both MDM2 isoforms coimmunoprecipitate with *RUNX3* (Fig. 2B), indicating that endogenous *RUNX3* interacts with endogenous MDM2.

**MDM2 downregulates RUNX3 protein levels.** We investigated whether MDM2 levels are inversely correlated not only with the levels of p53 but also with that of *RUNX3*. Epitope-tagged HA-*RUNX3* or HA-p53 were each coexpressed with increasing amounts of Flag-MDM2 in HEK-293 cells and the levels of the expressed proteins were monitored by immunoblotting. Strikingly, expression of MDM2 protein decreases the levels of both p53 and *RUNX3* (Fig. 2C). The complementary experiment in which MDM2 is depleted by siRNA administration reveals that a reduction in MDM2 increases endogenous *RUNX3* protein levels in both MKN45 gastric carcinoma cells and HEK-293 cells (Fig. 2D).

**Acidic domain of MDM2 mediates direct interactions with the Runt-homology domain of RUNX3.** To delineate the domains of *RUNX3* and MDM2 that are required for the interaction between the two proteins, serial deletion mutants of *RUNX3* and MDM2 were examined by immunoprecipitation-Western blot analysis (Supplementary Fig. S3A and C). Deletion of the *RUNX3* COOH-terminal region beyond amino acid 234 or the

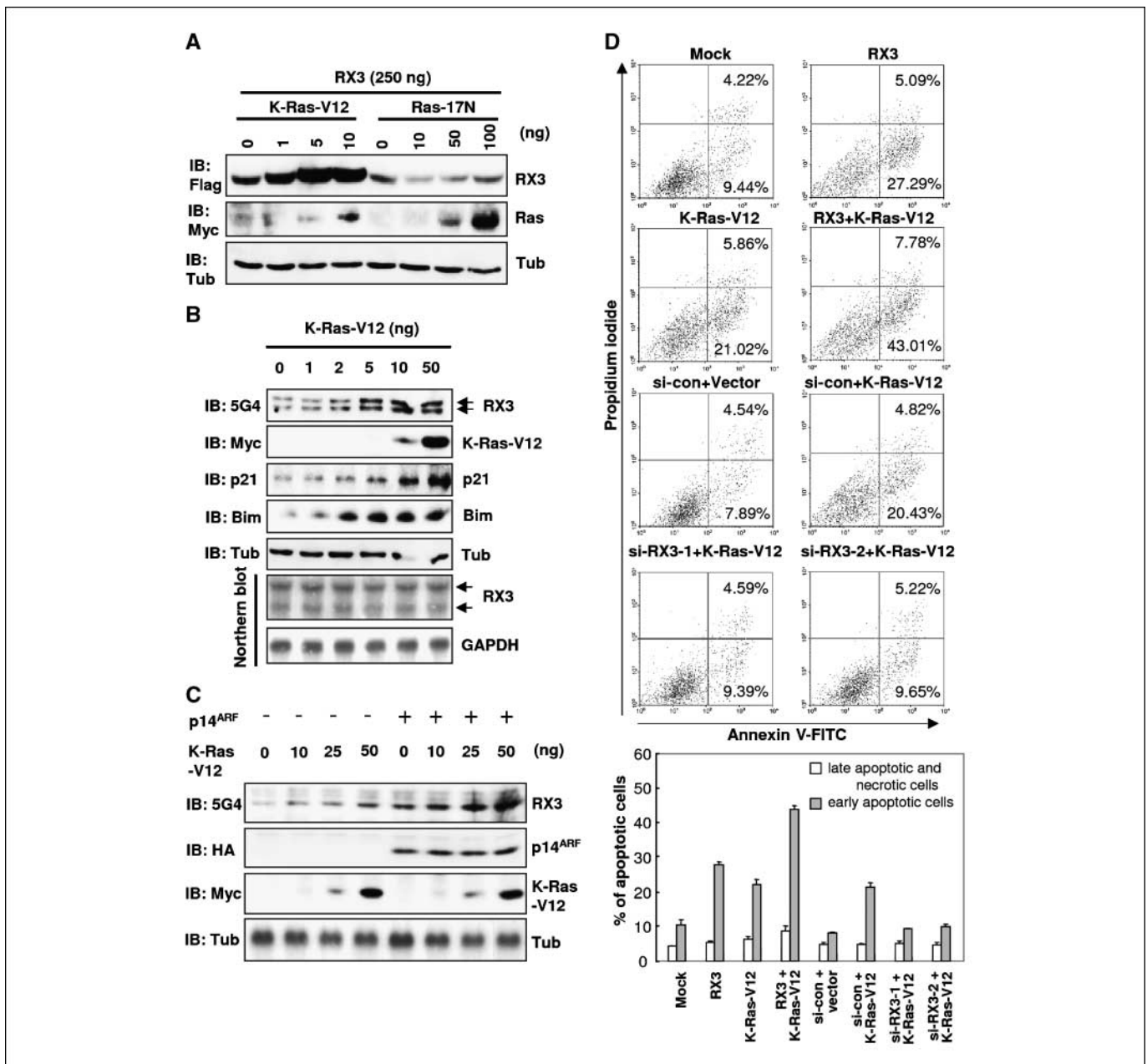


**Figure 1.** Ras activation elevates RUNX3 protein levels. *A*, Flag-RUNX3 was coexpressed with progressively increasing amounts of Myc-K-Ras-V12 or Myc-K-Ras-17N in HEK-293 cells, and levels of RUNX3 (RX3) and K-Ras (Ras) were measured by immunoblotting with anti-Flag or anti-Myc antibody. Tubulin (Tub) was immunoblotted with anti-tubulin antibody for loading control. *B*, progressively increasing amounts of Myc-K-Ras-V12 were expressed in HEK-293 cells, and levels of endogenous RUNX3, p21<sup>WAF/CIP</sup>, and Bim were assessed by immunoblotting with anti-RUNX3, anti-p21<sup>WAF/CIP</sup>, and anti-Bim antibody, respectively, and levels of RUNX3 mRNA were monitored by Northern blotting. *C*, serially increasing amounts of Myc-K-Ras-V12 were expressed with or without HA-p14<sup>ARF</sup> (250 ng) in A549 lung cancer cells that lack endogenous p14<sup>ARF</sup>. Endogenous level of RUNX3 was measured by anti-RUNX3 antibody. *D*, HEK-293 cells were transiently transfected with Myc-RUNX3, Myc-K-Ras-V12, and/or RUNX3-specific siRNAs. After 48 h transfection, cells were stained with Annexin V-FITC and propidium iodide. Apoptotic cells were detected by flow cytometry. The percentages of early apoptotic cells (Annexin V-FITC positive/propidium iodide negative; bottom right quadrant) and late apoptotic and necrotic cells (Annexin V-FITC positive/propidium iodide positive; top right quadrant) are shown. Results are summarized as a bar graph (bottom). Bars, SD of three independent experiments. IB, immunoblotting; IP, immunoprecipitation.

NH<sub>2</sub>-terminal region before amino acid 110 does not diminish binding to MDM2 (Supplementary Fig. S3B). However, removal of COOH-terminal region beyond amino acid 187 increased MDM2 binding. Deletion of the highly conserved Runt-homology domain between amino acids 54 and 187 abolishes interactions with MDM2. Taken together, these results indicate that the distal region of the Runt-homology domain (amino acids 110-187) is

essential for the RUNX3/MDM2 interaction and amino acids 187 to 234 inhibit the binding.

Complementary immunoprecipitation-Western blot experiments were done with full-length RUNX3 and MDM2 protein deletion mutants to define the domain of MDM2 that interacts with RUNX3. Deletion mutants encompassing the acidic domain of MDM2 were capable of binding full-length RUNX3, but deletion mutants lacking

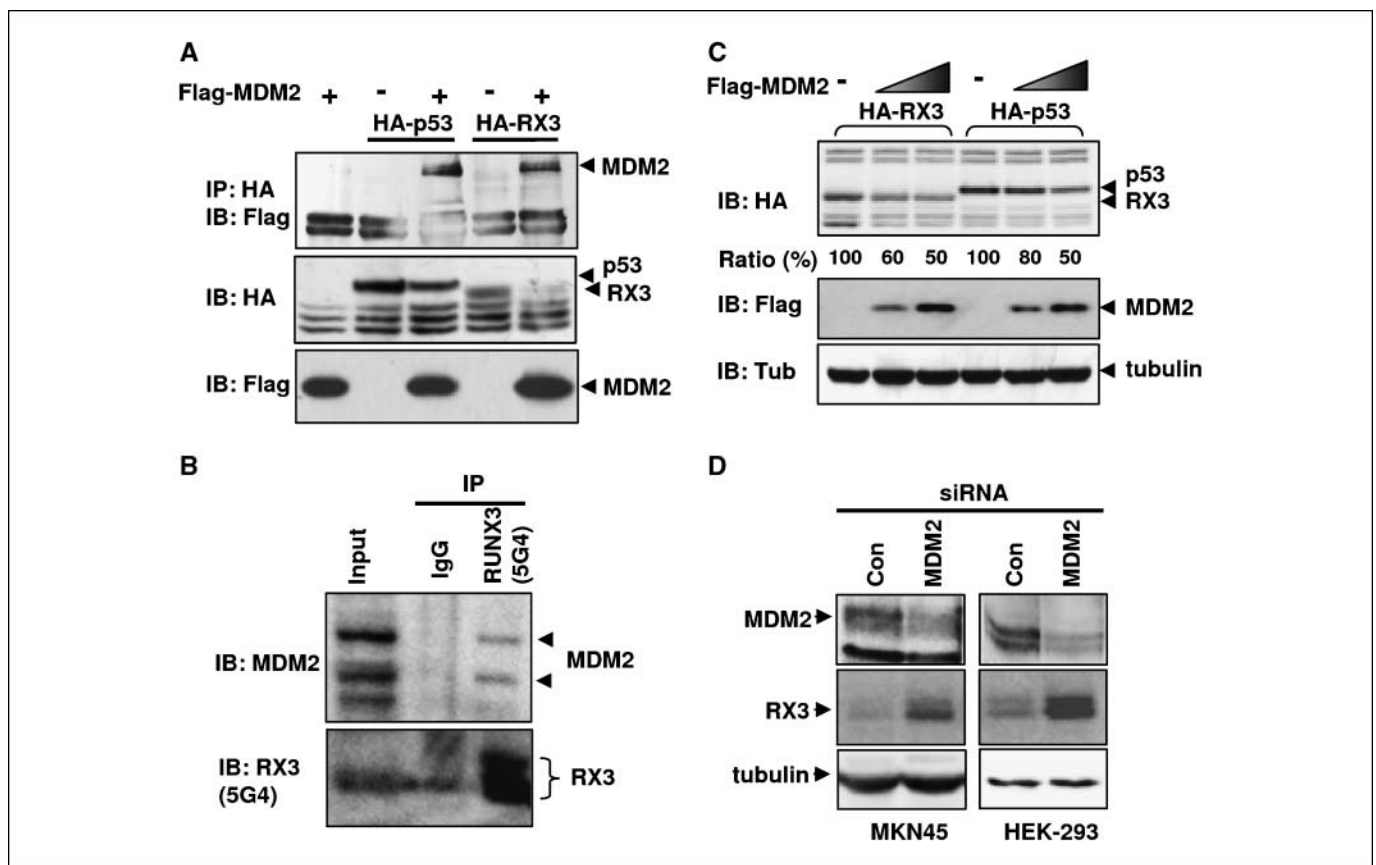


**Figure 2.** MDM2 physically interacts with RUNX3 and downregulates its protein level. *A*, *Flag-MDM2* was coexpressed with *HA-RUNX3* (*HA-RX3*) or *HA-p53* in HEK-293 cells, and cell lysates (500  $\mu$ g) were immunoprecipitated with anti-HA antibody and immunoblotted with anti-Flag antibody. Expression of transfected genes was detected by immunoblotting with anti-HA or anti-Flag antibody. *B*, cell lysate (1 mg) was obtained from MKN45 cells and immunoprecipitated with anti-RUNX3 monoclonal antibody (5G4) or IgG. The immunoprecipitate was analyzed by immunoblotting using anti-MDM2 antibody or anti-RUNX3 antibody. Input, 50  $\mu$ g of cell lysate for control. *C*, HEK-293 cells were transiently transfected with fixed amount of *HA-RUNX3* (0.4  $\mu$ g) or *HA-p53* (0.4  $\mu$ g) with an increasing amount of *Flag-MDM2* (0, 1.0, and 2.0  $\mu$ g). Protein expression levels were analyzed by immunoblotting using anti-HA or Flag antibody. The intensity of each band was quantitated by densitometry and the relative ratios are indicated. *D*, MKN45 and HEK-293 cells were treated with *siMDM2* and the endogenous levels of MDM2 and RUNX3 were examined by immunoblotting using anti-MDM2 antibody or anti-RUNX3 antibody.

this domain were not (Supplementary Fig. S3C and D). This result suggests that the acidic domain of MDM2 is essential for binding to RUNX3. Notably, deletion of NH<sub>2</sub>-terminal region, which interacts with p53, is dispensable for the MDM2/RUNX3 interactions. Thus, MDM2 interacts with p53 and RUNX3 through separate regions.

Because CBF $\beta$ , a heterodimeric partner of all three RUNX proteins, recognizes the conserved Runt domain, we examined whether CBF $\beta$  interferes with the interaction between RUNX3 and MDM2. Expression of fixed amounts of *RUNX3* and *MDM2* and progressively increasing amounts of *CBF $\beta$ 2* followed by immunoprecipitation-Western blot analysis revealed that CBF $\beta$ 2 does not interfere with the RUNX3-MDM2 interaction (Supplementary Fig. S4).

**MDM2 ubiquitinates RUNX3.** The RING finger domain of MDM2 represents the active site for its E3 ubiquitin ligase activity and mediates the ubiquitination of MDM2 itself and the pRB and p53 tumor suppressors (33). To determine whether RUNX3 is also a target of the E3 ubiquitin ligase activity of MDM2, we performed *in vivo* ubiquitination assays. A mutant MDM2 protein (C438A) that lacks ubiquitin ligase activity was used as a negative control. Flag-tagged wild-type and C438A mutant MDM2 proteins were coexpressed with Myc-RUNX3 and HA-Ub. Immunoprecipitation-Western blot analysis results reveal that wild-type MDM2 efficiently ubiquitinates RUNX3, but ubiquitination of RUNX3 by the

MDM2(C438A) mutant is severely reduced (Fig. 3A). The ubiquitination activity of MDM2 on RUNX3 was further examined under physiologic conditions by a loss-of-function approach. MKN45 cells were treated with siRNA for *MDM2* or a nonsilencing RNA as control. Ubiquitination of endogenous RUNX3 is evident under control conditions but decreased on siRNA-mediated knockdown of MDM2 protein (Fig. 3B). Because p14<sup>ARF</sup> is a key negative regulator of MDM2, we tested whether p14<sup>ARF</sup> inhibits MDM2-mediated RUNX3 ubiquitination. The result revealed that MDM2-mediated ubiquitination of RUNX3 is significantly reduced on coexpression of p14<sup>ARF</sup> (Fig. 3C). These results suggest that RUNX3 is a direct target of E3-ubiquitin ligase activity of MDM2 and p14<sup>ARF</sup> negatively regulates MDM2-mediated RUNX3 ubiquitination.

**RUNX3 protein is ubiquitinated by MDM2 at Lys<sup>94</sup> and Lys<sup>148</sup>.** MDM2 conjugates ubiquitin on lysine residues within its target proteins. To define the location of key lysine residues that modulate RUNX3 stability, we examined which RUNX3 deletion mutants are degradable by MDM2. RUNX3 protein deletion mutants were expressed with or without MDM2 and steady-state protein levels were measured by immunoblotting (Fig. 4A). Full-length RUNX3 as well as all other deletion mutants including a mutant protein containing only the NH<sub>2</sub>-terminal domain from amino acids 1 to 187 was still downregulated by coexpression of

MDM2 protein. Although RUNX3(1-187) interacts with MDM2 more strongly than wild-type RUNX3 or several deletion mutants, this increased binding does not correlate with increased MDM2-mediated degradation. This result suggests that the COOH-terminal region or RUNX3 beyond amino acid 187 may be required for efficient MDM2-mediated RUNX3 degradation.

We deduced that lysines required for MDM2-mediated ubiquitination are located within the Runt-homology domain. To verify this assumption, we examined whether the Runt-homology domain is ubiquitinated *in vitro*. Ubiquitination analysis using a purified recombinant His-tagged protein spanning the Runt-homology domain of RUNX3 reveals that the Runt-homology domain is ubiquitinated by MDM2 as reflected by a distinct mobility shift (Fig. 4B). Unlike *in vivo* assays that exhibit polyubiquitination, *in vitro* assays only permit monoubiquitination on each lysine residue (34). Calculation of the relative molecular mass of the Runt-homology domain (~17 kDa) and the corresponding ubiquitinated form (~39 kDa) reveals that the difference in the two bands is ~22 kDa. Because ubiquitin has a molecular mass of ~8.5 kDa, the size difference suggests that ubiquitination of RUNX3 occurs at either two or three sites.

To pinpoint lysine residues responsible for ubiquitination of RUNX3, we substituted the five lysine residues located within the Runt-homology domain to arginines. At least three of these residues (K94, K129, and K148) are located on the surface of the Runt domain based on the three-dimensional structure of the protein (35). Full-length wild-type and lysine mutant RUNX3 were each coexpressed together with MDM2 in HEK-293 cells and sensitivity to MDM2-mediated degradation was examined. The results show that the single lysine mutant K94R is more resistant to MDM2-mediated degradation than lysine mutant K148R, whereas the K129R mutant is as sensitive as the wild-type RUNX3 protein (Fig. 4C). Combination of the K94R and K148R mutations (double-mutant K94R/K148R) generates a stable protein that is more resistant than the single-mutant K94R. Importantly, triple mutation of the three remaining lysine residues within the Runt-homology domain (K129R/K186R/K192R) results in a protein that is as sensitive to MDM2-dependent destabilization as the wild-type RUNX3 protein. Taken together, we conclude that K94 and K148 are key target residues for ubiquitination and K94 may represent the primary site.

We validated the importance of K94 and K148 in regulation of RUNX3 protein levels by *in vivo* ubiquitination analysis in HEK-293 cells. Mutation of K94 (K94R mutant) virtually abolishes ubiquitination by MDM2, whereas a single mutation of K148 (K148R mutant) merely reduces ubiquitination and mutation of K129 (K129R mutant) has no discernible effect (Fig. 4D). These results suggest that ubiquitination occurs primarily on K94 and secondarily on K148 of RUNX3. It is possible that the two modification events are linked and that ubiquitination of K94 may be required for the second ubiquitination at K148.

**MDM2 suppresses the transcriptional activity of RUNX3.** MDM2 inhibits p53-mediated transcriptional activity by direct binding to the DNA-binding motif of p53 and by ubiquitination of p53, which results in nuclear export to the cytoplasm. We therefore investigated whether MDM2 downregulates RUNX3-mediated transcriptional activity using the RUNX3-responsive *p21<sup>CIP1/WAF1</sup>* promoter fused to the luciferase reporter gene (29). We find that the transactivation activity of RUNX3 is suppressed by MDM2 in a dose-dependent manner (Fig. 5A). Interestingly, the suppression of RUNX3 activity by MDM2 is released by the coexpression of *p14<sup>ARF</sup>*

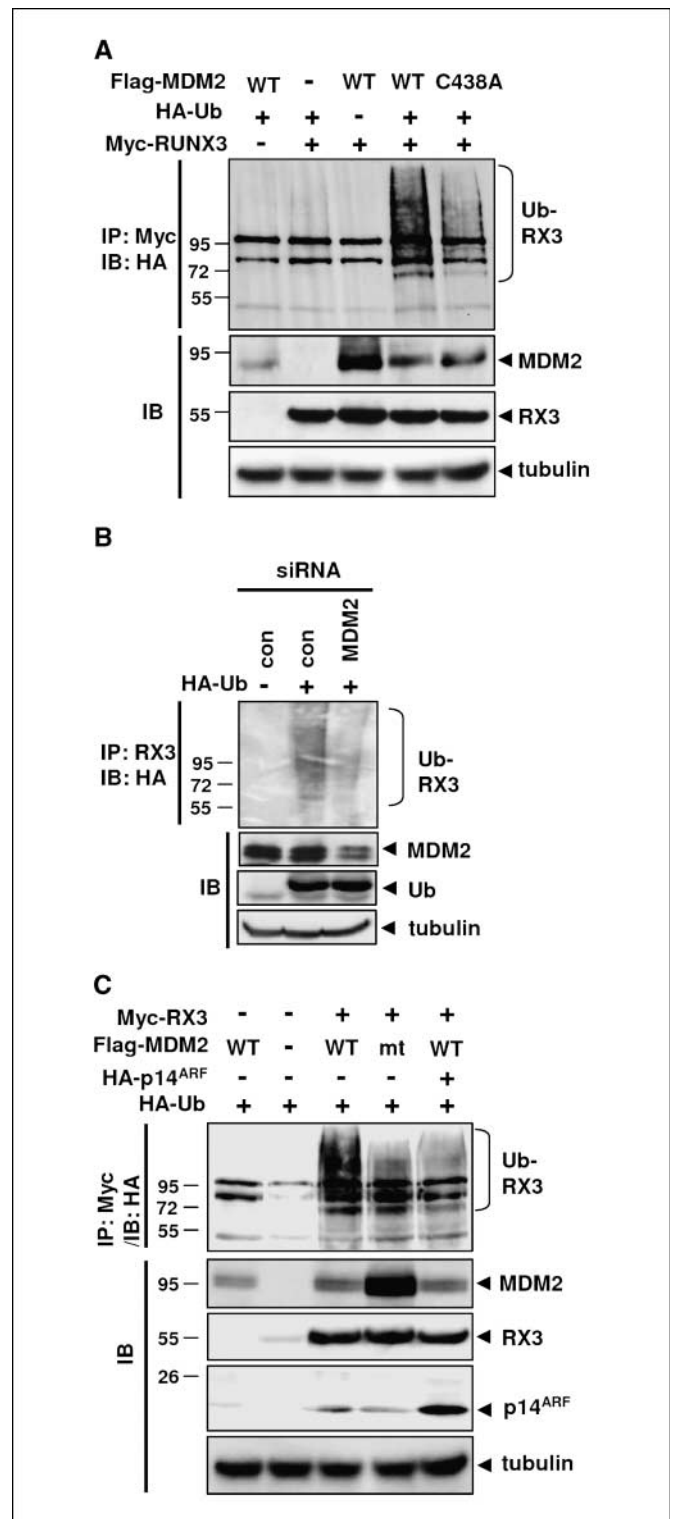


**Figure 3.** MDM2 facilitates ubiquitination of RUNX3 *in vivo*. **A**, Flag-MDM2 or mutant MDM2(C438A) was coexpressed with Myc-RUNX3 and HA-Ub in HEK-293 cells. Cell lysates (500  $\mu$ g for each reaction) were immunoprecipitated with anti-Myc (RUNX3) antibody and analyzed by immunoblotting with anti-HA (Ub) antibody. WT, wild-type. **B**, MKN45 cells were transfected with HA-Ub and MDM2 specific siRNA and the ubiquitination of endogenous RUNX3 was measured by immunoprecipitation with anti-RUNX3 antibody and immunoblotting with anti-HA (Ub) antibody. **C**, Flag-MDM2 (WT) or Flag-MDM2(C438A) (mt) was coexpressed with Myc-RUNX3, HA-Ub, and HA-p14<sup>ARF</sup>. Cell lysates (500  $\mu$ g for each reaction) were immunoprecipitated with anti-Myc (RUNX3) antibody and analyzed by immunoblotting with anti-HA (Ub) antibody.

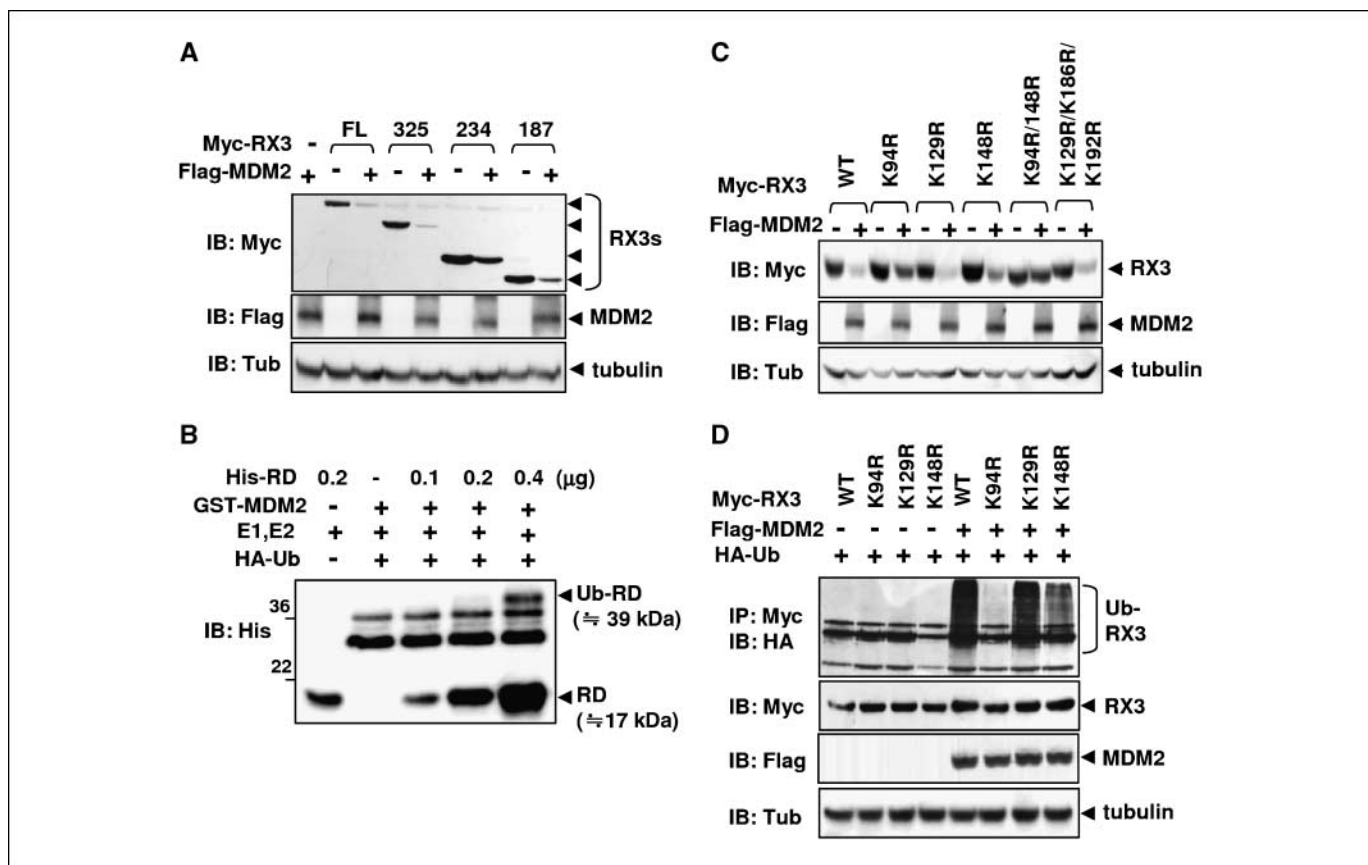


**Figure 4.** Identification of ubiquitination sites. *A*, *Myc-RUNX3* and its serial deletion constructs were coexpressed with *Flag-MDM2* in HEK-293 cells. Expression levels of transfected genes were measured by immunoblotting with anti-Myc or anti-Flag antibody. *B*, purified GST-MDM2 and His-Runt domain (*His-RD*; amino acids 64-190) were mixed with E1, E2, and HA-Ub for *in vitro* ubiquitination. His-Runt domain was analyzed by SDS-PAGE followed by immunoblotting with anti-His antibody. *C*, wild-type *RUNX3* and its lysine-to-arginine mutants (K94R, K129R, K148R, K94/148R, and KR-129,186,192) were expressed with or without *MDM2*, and protein levels were analyzed by immunoblotting using anti-Myc (*RUNX3*) and anti-Flag (*MDM2*) antibodies. *D*, *Myc-RUNX3* and its mutants (K94R, K129R, and K148R) and *HA-Ub* were coexpressed with or without *Flag-MDM2*. *RUNX3* ubiquitination was measured by immunoprecipitation with anti-Myc (*RUNX3*) antibody followed by immunoblotting with anti-HA (Ub) antibody.

(Fig. 5*B*). Reporter gene assays reveal that mutant *MDM2*(C438A), which lacks ubiquitin ligase activity, also inhibits *RUNX3* stimulation of *p21* promoter activity although less effectively than wild-type *MDM2* (Fig. 5*C*). This result suggests that the transcriptional activity of *RUNX3* is controlled by *MDM2* through an ubiquitination-independent mechanism. Consistent with this interpretation, the transactivating activity of the ubiquitination-defective mutant *RUNX3*-K94R is also suppressed by *MDM2* although not to the same extent as wild-type *RUNX3* (Fig. 5*D*). Collectively, these results suggest that, similar to p53, *RUNX3* is inactivated by *MDM2* by both ubiquitination-dependent destabilization and ubiquitination-independent interference with transcriptional activation.

**MDM2 facilitates nuclear export of *RUNX3*.** *MDM2* induces nuclear export of p53, which subsequently leads to the degradation of the protein. To investigate the possibility that *MDM2* also facilitates nuclear exclusion of *RUNX3*, we transiently transfected *Myc-RUNX3* and *Flag-MDM2* proteins in HeLa cells and analyzed the subcellular localization of *RUNX3* by immunofluorescence microscopy. *RUNX3* alone and *MDM2* alone are each exclusively localized in the nucleus (Fig. 6*A*), corroborating previous studies (36). However, when both genes are expressed within the same cell, *RUNX3* becomes localized in the cytoplasm, indicating export

from the nucleus (Fig. 6*B*). However, an ubiquitination-defective *MDM2* mutant (*MDM2*-339; see Supplementary Fig. S3), which lacks the RING finger domain, fails to translocate *RUNX3* to cytoplasm (Fig. 6*C*). Hence, the E3-ubiquitin ligase activity of *MDM2* is required for the cytoplasmic sequestration of *RUNX3*. Consistent with this observation, wild-type *MDM2* fails to translocate the ubiquitination-defective mutant *RUNX3*-K94R to the cytoplasm (Fig. 6*D*). Fractionated nuclear and cytoplasmic proteins from transfected cells expressing *RUNX3* and *MDM2* or *MDM2*-339 was examined by immunoblotting analysis. The results confirmed that *MDM2* but not *MDM2*-339 facilitates cytoplasmic localization of *RUNX3* (data not shown). Taken together, these results indicate that *MDM2* induces nuclear export of *RUNX3* through ubiquitination. We conclude that *MDM2* controls *RUNX3* through the same mechanisms as documented for p53.

## Discussion

*RUNX3* is a tumor suppressor and inactivation of its nuclear function is prevalent in various tumors. Here, we provide insight into a key mechanism by which *RUNX3* exerts its biological functions. Our data indicate that *RUNX3* is a principal lineage-specific component of the p14<sup>ARF</sup>-*MDM2* oncogenic surveillance pathway,

thus clarifying how deregulation of RUNX3 activity is linked to cancer susceptibility.

Unlike the ubiquitously expressed p53 protein, *RUNX3* is expressed in distinct tissues and regulate cell growth and differentiation in a lineage-specific manner. However, *RUNX3* has also many similarities with *p53*. For example, *RUNX3* and *p53* are very frequently inactivated in various kinds of tumors and the frequencies are ~50% (25, 37). Both *RUNX3* and *p53* are DNA-binding transcription factors that directly control the cell cycle and apoptosis (25). Both exert their growth-suppressive effects by regulating analogous molecular pathways; *RUNX3* is associated with its ability to induce cell cycle arrest and programmed cell death by transcriptional upregulation of the CDK inhibitor *p21<sup>CIP/WAF1</sup>* (29) and the apoptotic regulator *Bim* (*Bcl2L11*; ref. 30), respectively, and *p53* also controls *p21<sup>CIP/WAF1</sup>* and apoptotic mediators.

Although the *p53* pathway has a major role in the cellular protection mechanisms that prevent pathologic consequences of abnormal oncogenic stimulation (4), this pathway often fails to

respond to oncogene activation during cancer development. For example, *K-Ras* codon 12 mutation is frequently found at preneoplastic stages of lung adenocarcinoma, but *p53*-null mutations are found at even later stages (38, 39). This result suggests that there are *p53*-independent surveillance mechanisms that guard against unscheduled mitogenic cues. Interestingly, *RUNX3* is frequently downregulated in preneoplastic human lung adenocarcinomas (40). This result could possibly suggest that inactivation of *RUNX3* may be involved in *p53*-independent oncogene surveillance mechanisms.

In this study, we investigated how and when *RUNX3* is activated and found that *RUNX3* can be activated through *14<sup>ARF</sup>*-MDM2 pathway when *Ras* is abnormally activated. In normal conditions, MDM2 inactivates the transactivation activity of *RUNX3* through protein/protein interactions as well as mediates ubiquitination of *RUNX3* that stimulates nuclear export and subsequent degradation of *RUNX3*. Proteasomal degradation of *p53* is a staged event in which MDM2 and other E3 ubiquitin ligases (e.g., COP1 and Pirh2) ubiquitinate *p53* sequentially (41, 42).

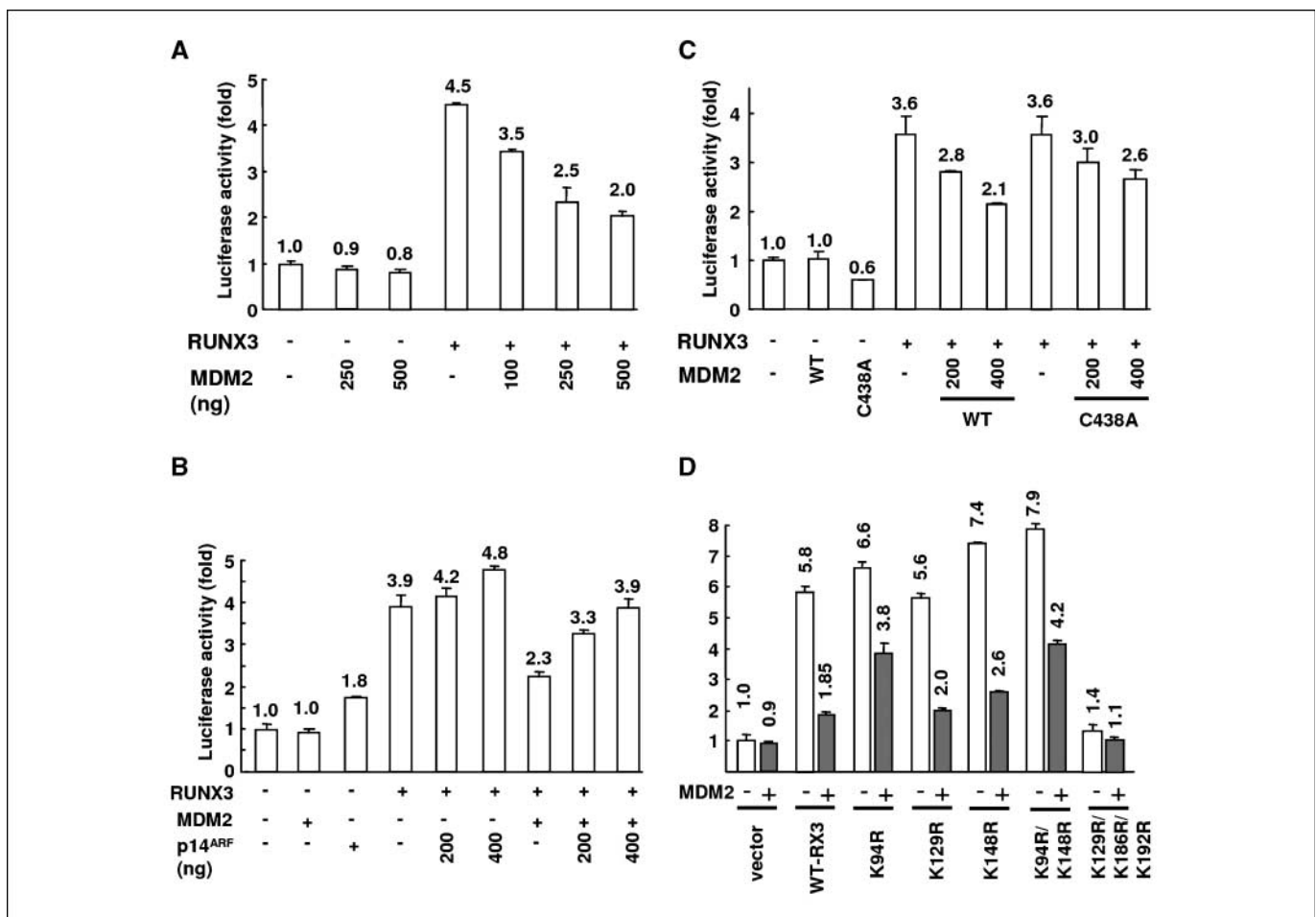


**Figure 5.** MDM2 inhibits RUNX3-mediated transcriptional activity. *A*, HEK-293 cells were transfected with a fixed amount of *RUNX3* (200 ng) and increasing amount of *MDM2* (100, 250, and 500 ng). The effect of *MDM2* on the transactivation activity of *RUNX3* was measured by the luciferase reporter assay. *B*, cells were transfected with fixed amount of *RUNX3* (200 ng) and *MDM2* (400 ng) and increasing amount of *p14<sup>ARF</sup>* (200 and 400 ng). The effect of *p14<sup>ARF</sup>* on the *MDM2*-mediated suppression of the *RUNX3* transactivation activity was measured by luciferase reporter assays. *C*, cells were transfected with a fixed amount of *RUNX3* (200 ng) and increasing amount of either wild-type *MDM2* or *MDM2(C438A)* (200 and 400 ng). The effect of the E3 ubiquitin ligase activity of *MDM2* on *RUNX3* transactivation activity was measured by the luciferase reporter assay. *D*, cells were transfected with wild-type *RUNX3* or lysine-mutated *RUNX3* and *MDM2*. Mutation of three lysine residues (K129R/K186R/K192R) by itself abolished *RUNX3* transactivation activity. The effect of *RUNX3* ubiquitination on its transactivation activity was measured by luciferase reporter assays using *pGL3-p21* promoter-luciferase (50 ng) as reporter and *pCMV- $\beta$ -gal* (50 ng) as internal control.

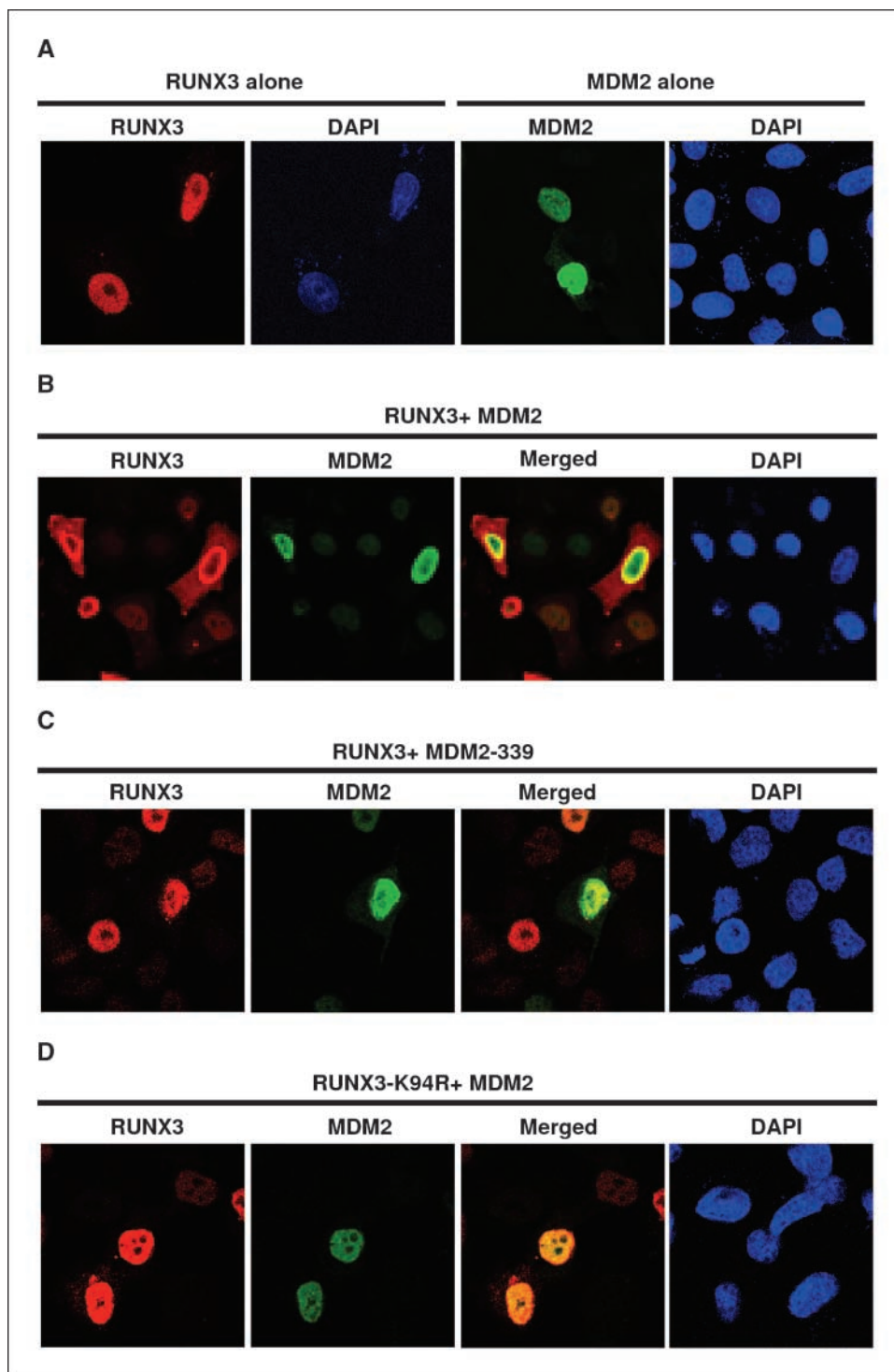


**Figure 6.** MDM2 facilitates nuclear export of RUNX3. HeLa cells were transfected with *Myc-RUNX3* and *Flag-MDM2* or their mutants. The subcellular localization of the expressed proteins was detected by immunofluorescent staining. Each nucleus was visualized by 4',6-diamidino-2-phenylindole (DAPI) staining. *A*, image of cells expressing *Myc-RUNX3* alone or *Flag-MDM2* alone. RUNX3 and MDM2 were detected exclusively in nucleus. *B*, image of cells coexpressing *Myc-RUNX3* and *Flag-MDM2*. Substantial level of RUNX3 was detected in cytoplasm in cells expressing *MDM2*. *C*, image of cells coexpressing *Myc-RUNX3* and *Flag-MDM2-339*. RUNX3 was detected only in the nucleus even in the cells expressing *MDM2-339*. *D*, image of cells coexpressing *Myc-RUNX3-K94R* and *Flag-MDM2*. RUNX3-K94R was detected only in the nucleus even in the cells expressing wild-type MDM2.

MDM2 stimulates nuclear export of p53 mainly through monoubiquitination or biubiquitination (43, 44). Our results show that MDM2 promotes nuclear export of RUNX3. Similar to p53, MDM2 may support monoubiquitination of Runx3 in the nucleus, thus promoting nuclear export and cytoplasmic polyubiquitination by other ubiquitin E3 ligases before proteasomal delivery.

The NH<sub>2</sub>-terminal region of MDM2 directly binds to p53 and inhibits transactivation by p53. This activity is independent of the

ability of MDM2 to reduce p53 levels through its COOH-terminal enzymatic domain (5). We found that MDM2 also inhibits RUNX3-mediated transcriptional activity in a concentration-dependent manner even if the ubiquitin-conjugating activity of MDM2 is compromised (C438A mutant). Thus, analogous to p53, MDM2 can inhibit RUNX3 activity through two separate functions: it promotes degradation of RUNX3 and can block transcriptional activation. Our data show that one key difference between p53 and RUNX3 is that the latter binds to the acidic domain of MDM2,

a region that is adjacent to the NH<sub>2</sub>-terminal domain of MDM2 that interacts with p53 and pRB (45, 46).

The p14<sup>ARF</sup>-MDM2-p53 pathway is subject to p53-dependent feedback regulation and resembles a molecular oscillator. *MDM2* gene transcription is activated by p53 as a normal part of the mechanisms that resolves a p53-dependent growth arrest in response to DNA damage or oncogenic stimuli. The linkage of this pathway to RUNX3 indicates that p53 can indirectly control RUNX3 levels. In conclusion, our results suggest involvement of RUNX3 in oncogene surveillance and a remarkable dual role for MDM2 in attenuating the levels of p53 and RUNX3 as principal tumor suppressors.

## References

1. Blyth K, Cameron ER, Neil JC. The RUNX genes: gain or loss of function in cancer. *Nat Rev Cancer* 2005; 5:376–87.
2. Bartek J, Lukas J, Mammalian G<sub>1</sub>- and S-phase checkpoints in response to DNA damage. *Curr Opin Cell Biol* 2001;13:738–47.
3. Brooks CL, Gu W. p53 ubiquitination: Mdm2 and beyond. *Mol Cell* 2006;21:307–15.
4. Efeyan A, Serrano M. p53: guardian of the genome and policeman of the oncogenes. *Cell Cycle* 2007;6:1006–10.
5. Leng P, Brown DR, Shivakumar CV, Deb S, Deb SP. N-terminal 130 amino acids of MDM2 are sufficient to inhibit p53-mediated transcriptional activation. *Oncogene* 1995;10:1275–82.
6. Cordon-Cardo C, Latres E, Drobnjak M, et al. Molecular abnormalities of mdm2 and p53 genes in adult soft tissue sarcomas. *Cancer Res* 1994;54:794–9.
7. Zou M, Shi Y, al-Sedairy S, Hussain SS, Farid NR. The expression of the MDM2 gene, a p53 binding protein, in thyroid carcinogenesis. *Cancer* 1995;76:314–8.
8. Dubs-Poterszman MC, Tocque B, Wasyluk B. MDM2 transformation in the absence of p53 and abrogation of the p107 G<sub>1</sub> cell-cycle arrest. *Oncogene* 1995;11:2445–9.
9. Sigalas I, Calvert AH, Anderson JJ, Neal DE, Lunec J. Alternatively spliced mdm2 transcripts with loss of p53 binding domain sequences: transforming ability and frequent detection in human cancer. *Nat Med* 1996;2:912–7.
10. Ito Y. Oncogenic potential of the RUNX gene family: 'overview'. *Oncogene* 2004;23:4198–208.
11. van Wijnen AJ, Stein GS, Gergen JP, et al. Nomenclature for Runt-related (RUNX) proteins. *Oncogene* 2004; 23:4209–10.
12. Look AT. Oncogenic transcription factors in the human acute leukemias. *Science* 1997;278:1059–64.
13. Osato M, Asou N, Abdalla E, et al. Biallelic and heterozygous point mutations in the runt domain of the AML1/PEBP2 $\alpha$ B gene associated with myeloblastic leukemias. *Blood* 1999;93:1817–24.
14. Speck NA, Gilliland DG. Core-binding factors in haematopoiesis and leukaemia. *Nat Rev Cancer* 2002;2: 502–13.
15. Komori T, Yagi H, Nomura S, et al. Targeted disruption of Cbfa1 results in a complete lack of bone formation owing to maturational arrest of osteoblasts. *Cell* 1997;89:755–64.
16. Otto F, Thornell AP, Crompton T, et al. Cbfa1, a candidate gene for cleidocranial dysplasia syndrome, is essential for osteoblast differentiation and bone development. *Cell* 1997;89:765–71.

## Disclosure of Potential Conflicts of Interest

No potential conflicts of interest were disclosed.

## Acknowledgments

Received 3/20/09; revised 7/27/09; accepted 8/15/09; published OnlineFirst 10/6/09.

**Grant support:** Creative Research Grant R16-2003-002-01001-02006 from the Korea Science and Engineering Foundation (S.-C. Bae) and NIH grants R01-AR49069 (A.J. van Wijnen) and P01-CA082834 (G.S. Stein).

The costs of publication of this article were defrayed in part by the payment of page charges. This article must therefore be hereby marked *advertisement* in accordance with 18 U.S.C. Section 1734 solely to indicate this fact.

We thank Jane Lian and Janet Stein for stimulating discussions.

17. Lee B, Thirunavukkarasu K, Zhou L, et al. Missense mutations abolishing DNA binding of the osteoblast-specific transcription factor OSF2/CBFA1 in cleidocranial dysplasia. *Nat Genet* 1997;16:307–10.
18. Mundlos S, Otto F, Mundlos C, et al. Mutations involving the transcription factor CBFA1 cause cleidocranial dysplasia. *Cell* 1997;89:773–9.
19. Thomas DM, Johnson SA, Sims NA, et al. Terminal osteoblast differentiation, mediated by runx2 and p27<sup>KIP1</sup>, is disrupted in osteosarcoma. *J Cell Biol* 2004; 167:925–34.
20. Taniuchi I, Osato M, Egawa T, et al. Differential requirements for Runx proteins in CD4 repression and epigenetic silencing during T lymphocyte development. *Cell* 2002;111:621–33.
21. Woolf E, Xiao C, Fainaru O, et al. Runx3 and Runx1 are required for CD8 T cell development during thymopoiesis. *Proc Natl Acad Sci U S A* 2003;100:7731–6.
22. Inoue K, Ozaki S, Shiga T, et al. Runx3 controls the axonal projection of proprioceptive dorsal root ganglion neurons. *Nat Neurosci* 2002;5:946–54.
23. Levanon D, Bettoun D, Harris-Cerruti C, et al. The Runx3 transcription factor regulates development and survival of TrkC dorsal root ganglia neurons. *EMBO J* 2002;21:3454–63.
24. Bae SC, Choi JK. Tumor suppressor activity of RUNX3. *Oncogene* 2004;23:4336–40.
25. Li QL, Ito K, Sakakura C, et al. Causal relationship between the loss of RUNX3 expression and gastric cancer. *Cell* 2002;109:113–24.
26. Kim WJ, Kim EJ, Jeong P, et al. RUNX3 inactivation by point mutations and aberrant DNA methylation in bladder tumors. *Cancer Res* 2005;65:9347–54.
27. Ito K, Lim AC, Salto-Tellez M, et al. RUNX3 attenuates  $\beta$ -catenin/T cell factors in intestinal tumorigenesis. *Cancer Cell* 2008;14:226–37.
28. Weisenberger DJ, Siegmund KD, Campan M, et al. CpG island methylator phenotype underlies sporadic microsatellite instability and is tightly associated with BRAF mutation in colorectal cancer. *Nat Genet* 2006;38: 787–93.
29. Chi XZ, Yang JO, Lee KY, et al. RUNX3 suppresses gastric epithelial cell growth by inducing p21(WAF1/Cip1) expression in cooperation with transforming growth factor  $\beta$ -activated SMAD. *Mol Cell Biol* 2005;25:8097–107.
30. Yano T, Ito K, Fukamachi H, et al. The RUNX3 tumor suppressor upregulates Bim in gastric epithelial cells undergoing transforming growth factor  $\beta$ -induced apoptosis. *Mol Cell Biol* 2006;26:4474–88.
31. Kilbey A, Terry A, Cameron ER, Neil JC. Oncogene-induced senescence: an essential role for Runx. *Cell Cycle* 2008;7:2333–40.
32. Fuchs SY, Adler V, Buschmann T, Wu X, Ronai Z. Mdm2 association with p53 targets its ubiquitination. *Oncogene* 1998;17:2543–7.
33. Honda R, Yasuda H. Activity of MDM2, a ubiquitin ligase, toward p53 or itself is dependent on the RING finger domain of the ligase. *Oncogene* 2000;19:1473–6.
34. Lai Z, Ferry KV, Diamond MA, et al. Human mdm2 mediates multiple mono-ubiquitination of p53 by a mechanism requiring enzyme isomerization. *J Biol Chem* 2001;276:31357–67.
35. Tahirov TH, Inoue-Bungo T, Morii H, et al. Structural analyses of DNA recognition by the AML1/Runx-1 Runt domain and its allosteric control by CBF $\beta$ . *Cell* 2001;104: 755–67.
36. Gu J, Nie L, Kawai H, Yuan ZM. Subcellular distribution of p53 and p73 are differentially regulated by MDM2. *Cancer Res* 2001;61:6703–7.
37. Kim TY, Lee HJ, Hwang KS, et al. Methylation of RUNX3 in various types of human cancers and premalignant stages of gastric carcinoma. *Lab Invest* 2004;84:479–84.
38. Slebos RJ, Baas IO, Clement MJ, et al. p53 alterations in atypical alveolar hyperplasia of the human lung. *Hum Pathol* 1998;29:801–8.
39. Cazorla M, Hernández L, Fernández PL, et al. Ki-ras gene mutations and absence of p53 gene mutations in spontaneous and urethane-induced early lung lesions in CBA/J mice. *Mol Carcinog* 1998;21:251–60.
40. Licchese JD, Westra WH, Hooker CM, Machida EO, Baylin SB, Herman JG. Epigenetic alteration of Wnt pathway antagonists in progressive glandular neoplasia of the lung. *Carcinogenesis* 2008;29:895–904.
41. Dornan D, Wertz I, Shimizu H, et al. The ubiquitin ligase COP1 is a critical negative regulator of p53. *Nature* 2004;429:86–92.
42. Leng RP, Lin Y, Ma W, et al. Pirh2, a p53-induced ubiquitin-protein ligase, promotes p53 degradation. *Cell* 2003;112:779–91.
43. Li M, Brooks CL, Wu-Baer F, Chen D, Baer R, Gu W. Mono- versus polyubiquitination: differential control of p53 fate by Mdm2. *Science* 2003;302:1972–5.
44. Oh W, Lee EW, Sung YH, et al. Jab1 induces the cytoplasmic localization and degradation of p53 in coordination with Hdm2. *J Biol Chem* 2006;281: 17457–65.
45. Chen J, Marechal V, Levine AJ. Mapping of the p53 and mdm-2 interaction domains. *Mol Cell Biol* 1993;13: 4107–14.
46. Sdek P, Ying H, Zheng H, et al. The central acidic domain of MDM2 is critical in inhibition of retinoblastoma-mediated suppression of E2F and cell growth. *J Biol Chem* 2004;279:53317–22.

# Cancer Research

The Journal of Cancer Research (1916–1930) | The American Journal of Cancer (1931–1940)

## Runt-Related Transcription Factor RUNX3 Is a Target of MDM2-Mediated Ubiquitination

Xin-Zi Chi, Jiyeon Kim, Yong-Hee Lee, et al.

*Cancer Res* 2009;69:8111-8119. Published OnlineFirst October 6, 2009.

<b>Updated version</b>	Access the most recent version of this article at: doi: <a href="https://doi.org/10.1158/0008-5472.CAN-09-1057">10.1158/0008-5472.CAN-09-1057</a>
<b>Supplementary Material</b>	Access the most recent supplemental material at: <a href="http://cancerres.aacrjournals.org/content/suppl/2009/10/01/0008-5472.CAN-09-1057.DC1">http://cancerres.aacrjournals.org/content/suppl/2009/10/01/0008-5472.CAN-09-1057.DC1</a>

<b>Cited articles</b>	This article cites 46 articles, 15 of which you can access for free at: <a href="http://cancerres.aacrjournals.org/content/69/20/8111.full#ref-list-1">http://cancerres.aacrjournals.org/content/69/20/8111.full#ref-list-1</a>
<b>Citing articles</b>	This article has been cited by 3 HighWire-hosted articles. Access the articles at: <a href="http://cancerres.aacrjournals.org/content/69/20/8111.full#related-urls">http://cancerres.aacrjournals.org/content/69/20/8111.full#related-urls</a>

<b>E-mail alerts</b>	<a href="#">Sign up to receive free email-alerts</a> related to this article or journal.
<b>Reprints and Subscriptions</b>	To order reprints of this article or to subscribe to the journal, contact the AACR Publications Department at <a href="mailto:pubs@aacr.org">pubs@aacr.org</a> .
<b>Permissions</b>	To request permission to re-use all or part of this article, use this link <a href="http://cancerres.aacrjournals.org/content/69/20/8111">http://cancerres.aacrjournals.org/content/69/20/8111</a> . Click on "Request Permissions" which will take you to the Copyright Clearance Center's (CCC) Rightslink site.